A Journal of the Gesellschaft Deutscher Chemiker

Angewandte International Edition GDCh Chemie

www.angewandte.org

Accepted Article

Title: Sulfur-coordinated organoiridium(III) complexes exert anti-breast cancer activity via inhibiting Wnt/β-catenin signaling

Authors: Qi Sun, Yi Wang, Qiuxia Fu, Ai Ouyang, Shanshan Liu, Zhongyuan Wang, Zijie Su, Jiaxing Song, Qianling Zhang, Pingyu Zhang, and Desheng Lu

To be cited as: *Angew. Chem. Int. Ed.* 10.1002/anie.202015009

Link to VoR: https://doi.org/10.1002/anie.202015009

WILEY-VCH

10.1002/anie.202015009

WILEY-VCH

RESEARCH ARTICLE

Sulfur-coordinated organoiridium(III) complexes exert anti-breast cancer activity *via* inhibiting Wnt/β-catenin signaling

Qi Sun,[a] Yi Wang,[b, c] Qiuxia Fu,[a] Ai Ouyang,[b] Shanshan Liu,[a] Zhongyuan Wang,[a] Zijie Su,[a] Jiaxing Song,[a] Qianling Zhang,[b] Pingyu Zhang,*[b] and Desheng Lu*[a]

Abstract: The sulfur-coordinated organoiridium(III) complexes **pbtIrSS** and **ppyIrSS**, which contain C,N and S,S (dithione) chelating ligands, are found to inhibit breast cancer tumorigenesis and metastasis *via* targeting Wnt/β-catenin signaling for the first time. Treatment with **pbtIrSS** and **ppyIrSS** induce the degradation of LRP6, thereby decreasing the protein levels of DVL2, β-catenin and activated β-catenin, resulting in downregulation of Wnt target genes CD44 and survivin. Additionally, **pbtIrSS** and **ppyIrSS** can suppress cell migration and invasion of breast cancer cells. Furthermore, both complexes show the ability to inhibit sphere formation and mediate stemness properties of breast cancer cells. Importantly, **pbtIrSS** exerts potent anti-tumor and anti-metastasis effects in mouse xenograft models through the blockage of Wnt/β-catenin signaling. Taken together, our results indicate that **pbtIrSS** has great potential to be developed as a breast cancer therapeutic agent with a novel mechanism.

Introduction

Breast cancer is the most commonly diagnosed cancer and the second leading cause of cancer death in women worldwide.[1] Although advanced therapeutic regimens have significantly improved overall survival in patients with breast cancer, there are still 20%-30% of patients with recurrence and 60% recurrent patients with metastasis. Increasing evidences suggest that the survival of cancer stem cells (CSCs) is a major cause of recurrence and metastasis in breast cancer. CSCs are a small subpopulation which possess self-renewal and differentiation potential.[2] The development of targeting therapy against breast CSCs may be a promising strategy for the treatment of breast cancer.

The Wnt signaling pathway is a highly conserved signaling system in biological evolution and plays an important role in organism development, stem cell function and tissue homeostasis.[3] The abnormal activation of Wnt signaling pathway is closely related to the maintenance of CSCs and the development of multiple tumors, including breast cancer.[4] The multifunctional protein β-catenin is a key component of this pathway, and its protein levels are controlled by a destruction complex, which consists of scaffolding protein Axin, Adenomatous polyposis coli (APC), Casein kinase 1 (CK1) and Glycogen synthase kinase 3β (GSK3β). CK1 and GSK3β phosphorylate β-catenin, promoting degradation of β-catenin through the ubiquitin-proteasome pathway. Wnt ligands bind to a Frizzled receptor (Fzd) as well as the co-receptors low density lipoprotein receptor-related protein 5/6 (LRP5/6), resulting in the recruitment of the β-catenin destruction complex to the LRP receptors and subsequent phosphorylation of one or more cytoplasmic motifs of LRP5/6. This event induces the activation of Dishevelled (DVL) and the inhibition of GSK3β. Unphosphorylated β-catenin accumulates in cytoplasm and translocates into the nucleus. By interacting with T-cell factor/lymphoid enhancing factor (TCF/LEF) transcription factors, β-catenin displaces the corepressors and recruits the transcriptional Kat3 coactivators p300 and/or CREB-binding protein (CBP), finally resulting in the expression of Wnt target genes, such as CD44, cyclin D1, c-Myc, survivin, and fibronectin.[5]

Metal-based drug cisplatin is one of the most widely used chemotherapeutic agent for various types of cancers. The anticancer activity of cisplatin is associated with its ability to crosslink with the guanine residues on the DNA, leading to DNA damage in cancer cells.[6] However, its clinical efficacy is largely limited by numerous side effects, drug resistance and limited spectrum of activity.[7] This has prompted the exploration of other metal-based anticancer drugs and their potential targets in cancer cells.[8] The main challenge concerning the improvement of therapy is to develop more metal complexes with ability to selectively target cancer-associated signaling pathways. As far as we know, very little is known about the effects of metal-based complexes on the Wnt signaling pathway.

Recently, iridium(III)-based complexes have attracted increasing attention because of their potent anticancer activities, limited side effects and improved selectivity towards cancer cells.[9] Iridium(III) complexes elicit their biological activity through different mechanisms from platinum-based drugs. Previous studies have demonstrated that iridium(III) complexes could trigger the production of intracellular reactive oxygen species (ROS) levels, reduce the mitochondrial membrane potential and cause a series of cell death-related events mediated by mitochondria.[10f,g] Sadler et al. reported on a luminescent iridium(III) complex inducing NADH depletion, ROS generation,

[a] Dr. Q. Sun, Q. Fu, S. Liu, Z. Wang, Z. Su, J. Song, Prof. Dr. D. Lu
Guangdong Key Laboratory for Genome Stability & Disease Prevention, International Cancer Center, Department of Pharmacology, Shenzhen University Health Science Center
Shenzhen, 518060, China
E-mail: delu@szu.edu.cn
[b] Dr. P. Zhang, Y. Wang, A. Ouyang, Prof. Dr. Q. L. Zhang, College of Chemistry and Environmental Engineering, Shenzhen University
Shenzhen, 518060, P. R. China
E-mail:p.zhang6@szu.edu.cn
[c] Y. Wang, Key Laboratory for Advanced Materials of MOE, School of Chemistry & Molecular Engineering, East China University of Science and Technology
Shanghai, 200237, P. R. China
Supporting information for this article is given via a link at the end of the document.

intracellular redox imbalance and immunogenic apoptotic cancer cell death.[10] Mao et al. showed that cyclometalated iridium(III) complexes served as anion transporters mainly through an anion exchange mechanism to regulate lysosomal pH, leading to the inhibition of autophagic flux.[11] Moreover, the Ca^{2+}-binding protein calmodulin (CaM) has been identified as a target protein of iridium complexes. Several cationic amphiphilic tris-cyclometalated iridium(III) complexes were studied to interact with Ca^{2+}-CaM complex and then induce cell death.[12] In addition, some cyclometalated iridium(III) complexes have shown to induce apoptosis in breast CSC-enriched HMLER-shEcad cells through targeting mitochondria.[13] These compounds inhibited mammosphere formation to a similar extent as salinomycin. Salinomycin, an antibiotic potassium ionophore, has been reported to act as a selective breast CSC inhibitor. It inhibits the Wnt signaling pathway and exerts anticancer activity *in vitro* and *in vivo*.[14] So far, the mechanism underlying the anti-CSC properties of iridium complexes remain unclear. In this study, we synthesized four iridium(III) complexes, **pbtIrSS**, **ppyIrSS**, **pbtIrOO** and **ppyIrOO** (Scheme 1A), and explored their effects on Wnt/β-catenin signaling, cell viability, apoptosis, migration, invasion, and stemness in breast cancer cells. Their effects on breast tumor growth and lung metastasis were evaluated using mouse xenograph models. Our results demonstrated that **pbtIrSS** and **ppyIrSS** but not **pbtIrOO** and **ppyIrOO** exerted anti-tumor and anti-metastatic activities in breast cancer cells via inhibiting Wnt/β-catenin signaling and CSCs (Scheme 1B).

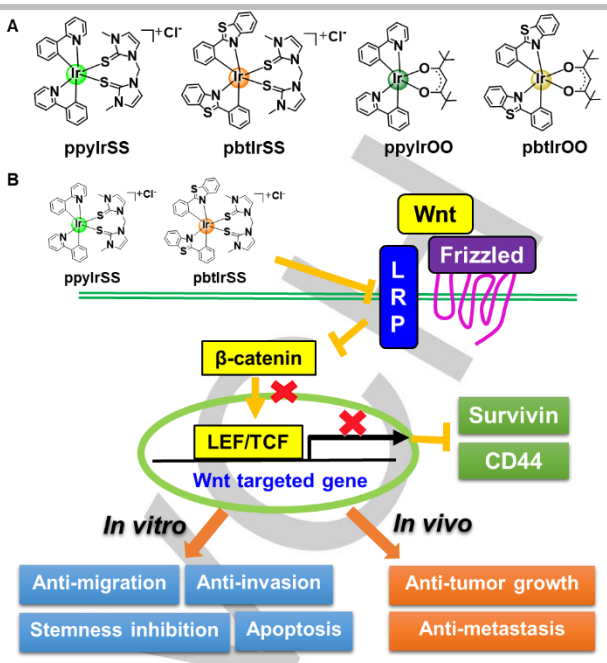

Scheme 1. (A) The chemical structures of the iridium(III) complexes studied in this work. (B) **pbtIrSS** and **ppyIrSS** exhibits potent anti-breast cancer activity *in vitro* and *in vivo* via blocking Wnt/β-catenin signaling.

Results and Discussion

The compounds were obtained in a high yield from the reaction of iridium dimer $[(ppy)_4Ir_2Cl_2]$ or $[(pbt)_4Ir_2Cl_2]$ (ppy: 2-phenylpyridine, pbt: 2-phenyl-1,3-benzo-thiazole) with 2 equiv. of S,S dithione ligand or 2,2,6,6-tetramethyl-3,5-heptanedione, respectively. As shown in Scheme 1A, both **ppyIrSS** and **pbtIrSS** had a unit positive charge, while **ppyIrOO** and **pbtIrOO** were neutral. This probably makes a difference in biological properties. Details of the synthesis were showed in the experimental section and Scheme S1. These compounds were characterized by the high-resolution mass spectrometry (Figures S1-S4), ^{1}H NMR (Figures S5-S8), ^{13}C NMR, (Figures S9-S12) and elemental analysis. In addition, the structures of **ppyIrOO** and **pbtIrOO** were studied by X-ray crystallography (Scheme S2). The crystallographic data, selected bond lengths and angles were listed in Tables S1-S2. The crystal structures showed that the Ir-O bond lengths ranged from 2.13 to 2.15 Å and the twist angles of O-Ir-O were around 87°.

The stabilities of the iridium(III) complexes in the PBS solution were monitored using UV-vis abosorption spectroscopy and high performance liquid chromatography (HPLC). The results showed that the iridium(III) complexes were highly stable for 72 h in the PBS solution (Figures S13-S14). The logarithm of the octanol-water partition coefficient (log $P_{o/w}$) is a measure of lipophilicity. As shown in Figure S15, **ppyIrSS** and **pbtIrSS** (log P = +2.05 for **ppyIrSS** and log P = +2.61 for **pbtIrSS**) were more lipophilic than **ppyIrOO** and **pbtIrOO** (log P = +0.63 for **ppyIrOO** and log P = +0.68 for **pbtIrOO**). The higher positive log $P_{o/w}$ value implied that this molecule might be more readily incorporated into cells.[9a]

The cellular uptake of the iridium complexes in living cells was investigatied using confocal laser scanning microscopy and inductively coupled plasma mass spectrometry (ICP-MS). MDA-MB-231 cells were treated with 2.5 μM iridium complexes for 1 h and then subjected to confocal imaging. As shown in Figure S16A, **ppyIrSS** and **pbtIrSS** showed a wide range of strong luminescence in the cells, while **ppyIrOO** and **pbtIrOO** exhibited only a small amount of spot-like luminescence. The cellular uptake amounts of these iririum(III) complexes were further quantitatively studied by ICP-MS (Figure S16B). The results showed that **ppyIrSS** and **pbtIrSS** had a six to ten-fold higher uptake than **ppyIrOO** and **pbtIrOO** across the cells. Thus, the cellular uptake of S,S compounds was more efficient than that of the O,O compounds.

We first examined the effect of these iridium(III) complexes on biological behaviours of breast cancer cells. The cytotoxicity of **pbtIrSS**, **ppyIrSS**, **pbtIrOO**, **ppyIrOO** and cisplatin was detected by a MTT assay. The complexes **pbtIrSS** and **ppyIrSS** exerted the strong cytotoxic potency compared with other compounds, with IC_{50} values of **pbtIrSS** at 1.30 ± 0.02 μM in MDA-MB-231 cells and at 0.89 ± 0.09 μM in MDA-MB-468 cells, IC_{50} values of **ppyIrSS** at 1.77 ± 0.13 μM in MDA-MB-231 cells and at 1.70 ± 0.15 μM in MDA-MB-468 cells (Figure 1A and B). Flow cytometry was used to analyze the apoptosis in MDA-MB-231 and MDA-MB-468 cells. The compounds **pbtIrSS** and **ppyIrSS** exhibited the potent pro-apoptotic effect in both cell lines (Figure 1C and D). These results revealed that **pbtIrSS** and **ppyIrSS** have more potent ability to induce apoptosis and inhibit cell viability in breast cancer cells than **pbtIrOO**, **ppyIrOO** and cisplatin. We further tested the effects of **pbtIrSS** and **ppyIrSS** on the migratory and invasive activities of MDA-MB-231 and MDA-MB-468 cells using transwell migration and invasion assays. The results showed that treatment with **pbtIrSS** and **ppyIrSS** (Figure S17A-D) significantly reduced the numbers of migrated and invaded cells in both cell lines, suggesting that **pbtIrSS** and **ppyIrSS** could attenuate the migratory and invasive ability of breast cancer cells. As a positve control, salinomycin also effectively induced the apoptosis and

10.1002/anie.202015009

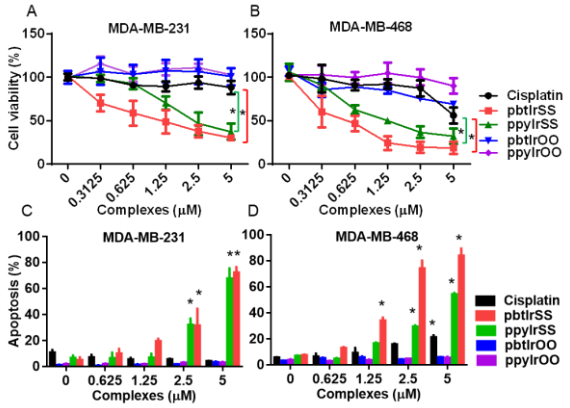

Figure 1. The iridium(III) complex pbtIrSS potently promotes apoptosis and suppresses viability in breast cancer cells. MDA-MB-231(A and C) MDA-MB-468 (B and D) cells were treated with iridium(III) complexes or cisplatin, respectively. (A and B) The cell viability was examined using the MTT assay. (C and D) Cell apoptosis was detected by FACS. Statistical analysis was conducted using one-way ANOVA followed by a Dunnett-t test. *P < 0.05 compared to vehicle control.

inhibited the viability, migration and invasion of breast cancer cells (Figure S18A-F). The IC_{50} values of salinomycin for MDA-MB-231 and MDA-MB-468 cell lines were 1.11 ± 0.12 μM and 1.35 ± 0.28 μM, respectively, showing comparable potency to pbtIrSS and ppyIrSS (Figure 1A and B, Figure S18A and B). However, cisplatin, a commonly used metal cancer chemotherapeutic drug, had little effect on these biological behaviour in breast cancer cells at the same concentrations (Figure1A-D, Figure S17E and F).

Cyclometalated iridium(III) complexes have been reported as anti-CSC agents.[14] Concerning the crucial role of Wnt/β-catenin signaling in the survival and maintenance of CSCs, we examined the effect of these iridium complexes on Wnt/β-catenin signaling. A SuperTopFlash reporter was transfected into HEK293T cells along with Wnt1, LRP6, Wnt1/LRP6, DVL2 or β-catenin expression plasmids, respectively. Treatment with 0.625-5 μM **pbtIrSS** (Figure 2A-D) and **ppyIrSS** (Figure S19A-D) dose-dependently inhibited the transcriptional activity of the SuperTopFlash reporter activated by Wnt1, LRP6, Wnt1/LRP6, and DVL2. However, **pbtIrOO** (Figure S20A-D) and **ppyIrOO** (Figure S20E-H) had little effect on the SuperTopFlash activity induced by Wnt1, LRP6, DVL2 and β-catenin. Furthermore, **pbtIrSS** and **ppyIrSS** did not inhibit the SuperTopFlash activity induced by β-catenin, indicating that **pbtIrSS** and **ppyIrSS** may act on the upstream elements of β-catenin (Figure 2E and Figure S19E). To examine the effect of **pbtIrSS** and **ppyIrSS** on other signaling pathways, we performed the transfection assays using an NFAT reporter (NFAT-Luc) and an AP1 reporter (AP1-Luc). The expression plasmids encoding NFATc and Ras^{V12} were used to activate the NFAT and AP1 signaling pathways in HEK293T cells, respectively. As shown in Figure 2F and G, Figure S19F and G, **pbtIrSS** and **ppyIrSS** had no inhibitory effects on the luciferase activities of NFAT-Luc and AP1-Luc. Salinomycin, an inhibitior of the Wnt signaling pathway, specifically inhibited the transcriptional activity of the SuperTopFlash reporter activated by the components of Wnt signaling (Figure S21A-G). In contrast, we did not observe any inhibitory effect of cisplatin on the transcriptional activity of the SuperTopFlash reporter at any of the concentrations tested (0.625-10 μM or 5-40 μM) (Figure S22). To further assess the effect of these iridium(III) complexes on the components of the Wnt/β-catenin signaling pathway, a Wnt1

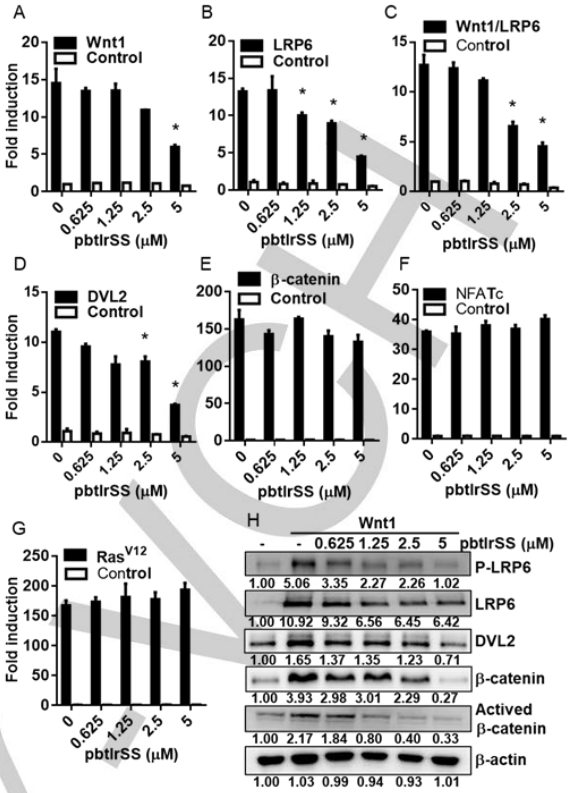

Figure 2. The iridium(III) complex pbtIrSS suppresses Wnt/β-catenin signaling. (A-D) HEK293T cells were transfected with SuperTopFlash reporter gene together with empty vector or expression plasmids encoding Wnt1 (A), LRP6 (B), Wnt1/LRP6 (C), DVL2 (D), and β-catenin (E). (F-G) HEK293T cells were transfected with NFAT-Luc reporter (F) together with NFATc expression plasmid, or AP-1-Luc reporter (G) along with constitutively active Ras^{v12} expression plasmid. The transfected cells were treated with vehicle control (DMSO) or **pbtIrSS**. Data were expressed as fold induction relative to vehicle control. Statistical analysis was conducted using one-way ANOVA followed by a Dunnett-t test. *P<0.05 versus vehicle control. (H) The expression levels of indicated components of Wnt signaling were detected by western blotting.

expression plasmid was transfected into HEK293T cells. After transfection for 24 h, the cells were treated with the increasing concentrations of **pbtIrSS** and **ppyIrSS**. Figure 2H and Figure S19H showed that expression of Wnt1 enhanced the levels of β-catenin, demonstrating the activation of the Wnt/β-catenin signaling pathway in HEK293T cells. Similar to salinomycin (Figure S21H), **pbtIrSS** or **ppyIrSS** significantly downregulated the levels of phosphorylated LRP6, total LRP6, DVL2, total β-catenin and activated β-catenin in the cells transfected with Wnt1 expression vector (Figure 2H and S19H). Taken together, our results illustrate that the iridium(III) complexes **pbtIrSS** and **ppyIrSS** can specifically inhibit Wnt/β-catenin signaling in HEK293T cells.

Increasing evidences have demonstrated that Wnt/β-catenin signaling is activated in different subtypes of human breast cancer. Several Wnt ligands, FZD receptors and LRP6 have been detected in various breast cancer cell lines and primary tumor tissues. Multiple negative modulators of this pathway are downregulated in many breast tumor tissues. These negative modulators include SFRP1, SFRP2, SFRP5, WIF1, DKK1 and DKK3.[15] Moreover, increased levels of β-catenin have been

10.1002/anie.202015009

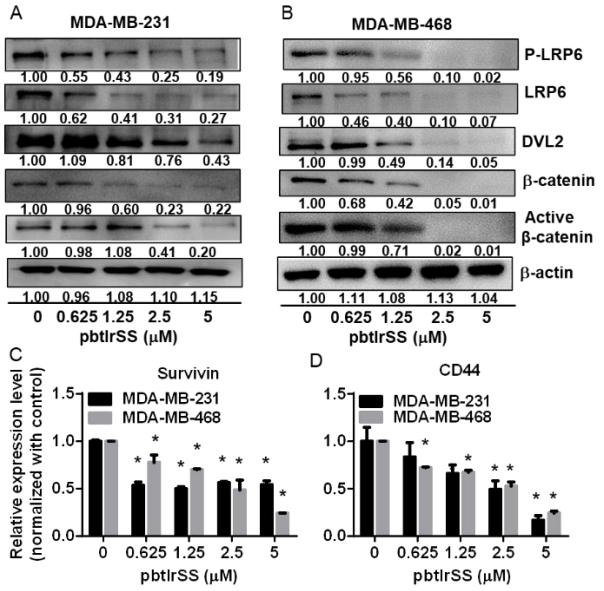

Figure 3. The iridium(III) complex pbtIrSS inhibits Wnt/β-catenin signaling in breast cancer cells. MDA-MB-231 and MDA-MB-468 cells were treated with **pbtIrSS**. (A and B) The expression levels of indicated components of Wnt signaling were analyzed by western blotting. The real-time PCR analysis was used to detect the mRNA expression of survivin(C) and CD44 (D). Statistical analysis was conducted using one-way ANOVA followed by a Dunnett-t test. *P < 0.05 compared to vehicle control.

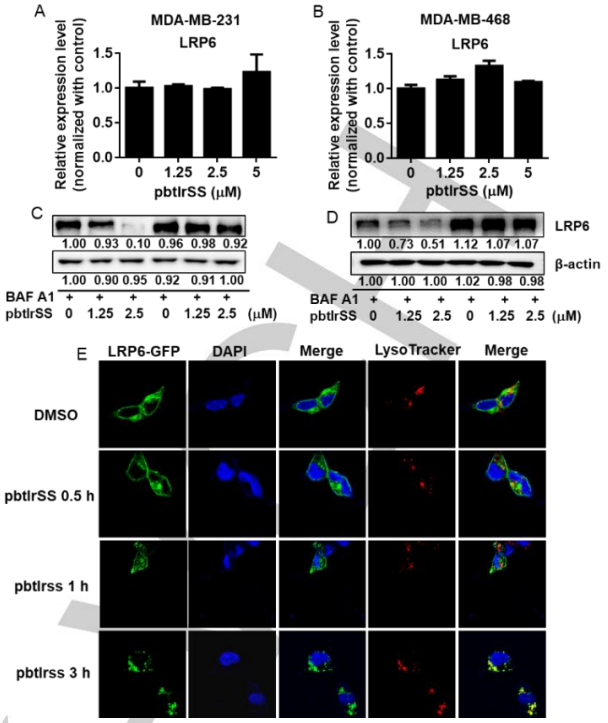

Figure 4. The iridium(III) complex pbtIrSS induces the internalization and degradation of LRP6 via a lysosome-dependent manner. The relative mRNA levels of LRP6 in **pbtIrSS**-treated MDA-MB-231 (A) and MDA-MB-468 (B) were detected by real-time PCR. MDA-MB-231 (C) and and MDA-MB-468 (D) cells were incubated with 1.25 or 2.5 μM **pbtIrSS** for 18 h before 10 nM BAF A1 was added. After incubation for another 6 h, the cells were harvested and the protein levels of LRP6 were detected by immunoblotting. (E) HEK293T cells were transfected with LRP6-GFP plasmid for 24 h. Then the cells were treated with vehicle or **pbtIrSS** before 70 nM Lyso Traker TM Deep Red was added. After incubation for indicated periods of time (0.5, 1 and 3 h), the cells were fixed and stained with DAPI.

observed in about 90% of breast tumors. To assess the effect of the iridium(III) complexes on Wnt/β-catenin signaling in breast cancer cells, MDA-MB231 and MDA-MB468 cells were transduced with lentiviral vectors encoding the 7xTCF-FFluc/SV40-mCherry (7TFC) reporter gene, which allow us to monitor Wnt/β-catenin activity using a luceferase assay. Treatment with **pbtIrSS**, **ppyIrSS** and salinomycin effectively inhibited the transcriptional activity of 7TFC Wnt reporter in MDA-MB-231 cells (Figure S23A-F) and MDA-MB-468 cells (Figure S23G-L). In contrast, **pbtIrOO**, **ppyIrOO** and cisplatin had no effect on Wnt signaling in both breast cancer cell lines. These results indicate that **pbtIrSS** and **ppyIrSS** could suppress Wnt/β-catenin signaling in breast cancer cells.

We further evaluated the effect of these iridium(III) complexes on the components of Wnt/β-catenin signaling in human breast cancer cells. MDA-MB-231 and MDA-MB-468 cells were treated with the increased doses of **pbtIrSS**, **ppyIrSS**, **pbtIrOO** and **ppyIrOO** for 24 h. The complexes **pbtIrSS** and **ppyIrSS** but not **pbtIrOO** and **ppyIrOO** remarkebly reduced the protein levels of phosphorylated LRP6, total LRP6, phosphorylated and unphosphorylated DVL2, total β-catenin and activated β-catenin in a dose-dependent manner (Figure 3A and B, Figure S24A-F). Survivin and CD44 are well-established Wnt target genes and are upregulated in breast cancer. Real-time PCR was employed to detect the expression of survivin and CD44. **pbtIrSS** and **ppyIrSS** at concentrations as low as 0.625 μM decreased mRNA expression of survivin and CD44 (Figure 3C and D, Figure S25A and B) in MDA-MB-231 and MDA-MB-468 cells. As expected, salinomycin not only decreased the expression of components of Wnt signaling (Figure S24G and H), but also downregulated the mRNA expression of survivin and CD44 (Figure S25C and D). However, cisplatin at dosed to 5 μM showed little inhibitory effects on the expression of Wnt signaling components (Figure S24I and J) and Wnt target genes (Figure S25E and F). These results indicate that **pbtIrSS, ppyIrSS** and salinomycin but not **pbtIrOO**, **ppyIrOO** and cisplatin have the ability to inhibit Wnt/β-catenin signaling in breast cancer.

In breast cancer, the components of Wnt signaling at the cell surface play an important role in the activation of this pathway. LRP6 is an essential Wnt co-receptor, whose expression is upregulated in various breast cancer cell lines and tumor tissues. Depletion of LRP6 in breast cancer cells remarkably suppressed Wnt/β-catenin signaling.[16] Overexpression of LRP6 in mammary epithelial cells is sufficient to activate Wnt/β-catenin signaling and induce mammary gland hyperplasia.[17] Our results showed **pbtIrSS** and **ppyIrSS** markedly downregulated the expression of LRP6 in HEK293T and breast cancer cells. We then test the effect of **pbtIrSS** and **ppyIrSS** on mRNA level of LRP6 in MDA-MB-231 and MDA-MB-468 cells. The real-time PCR results showed that treatment with **pbtIrSS** (Figure 4A and B) and **ppyIrSS** (Figure S26A and B) did not affect the mRNA expression of LRP6 in both cell lines, indicating that **pbtIrSS** and **ppyIrSS**-induced downregulation of LRP6 was independent of transcriptional regulation. To examine whether these two sulfur-coordinated organoiridium(III) complexes could enhance the degradation of LRP6, MDA-MB-231 and MDA-MB-468 cells were treated with the protein synthesis inhibitor cycloheximide (CHX) alone or combined with **pbtIrSS** or **ppyIrSS**. The results showed that treatment with CHX reduced the levels of endogenous LRP6 in a

time-dependent manner, and addition of **pbtIrSS** (Figure S27A and B) or **ppyIrSS** (Figure S26C and D) further accelerated the degradation of LRP6 protein in both cell lines. Next, the lysosome inhibitor bafilomycin A1 (BAF) and the proteasome inhibitor MG132 were used to determine the roles of lysosomal and proteasomal pathways in **pbtIrSS/ppyIrSS**-induced degradation of LRP6. In MDA-MB-231 and MDA-MB-468 cells, **pbtIrSS**-induced downregulation of LRP6 was significantly restored by treatment with BAF A1 (Figure 4C and D) but not by MG132 (Figure S27C and D). Similar to **pbtIrSS**, **ppyIrSS** also induced degradation of LRP6 in a BAF A1-mediated fashion (Figure S26E-H). Moreover, we observed that **pbtIrSS** and **ppyIrSS** could induce the internalization of LRP6 in a time-dependent manner (Figure 4E and Figure S26I). An increased lysosomal accumulation of LRP6 was observed following **pbtIrSS** or **ppyIrSS** treatment for 3 hours in HEK293T cells transfected with LRP6-GFP plasmid (Figure 4E and Figure S26I). These results indicated that **pbtIrSS/ppyIrSS**-induced degradation of LRP6 is regulated by the lysosomal pathway but not the proteasome pathway.

To explore the potential interaction between LRP6 protein and sulfur-coordinated iridium(III) complexes **pbtIrSS** and **ppyIrSS**, the luminescence intensities response of iridium(III) complexes were investigated in the presence of increasing concentrations of LRP6 protein. Figure S28A and B showed that the luminescence intensities of **pbtIrSS** and **ppyIrSS** increased in a LRP6 concentration-dependent manner. However, the luminescence intensities of **ppyIrOO and pbtIrOO** were almost kept unchanged under elevated LRP6 concentrations (Figure S28C and D). These results suggest that the sulfur-coordinated organoiridium(III) complexes are able to interact with LRP6 protein. Comparing the chemical structure of sulfur-coordinated complexes with **pbtIrOO** and **ppyIrOO**, the lipophilicity and type of charge of sulfur-coordinated complexes may contribute to their interaction with LRP6 protein. We further examined the colocalization of GFP-labeled LRP6 protein and iridium(III) complexes. LRP6-GFP expression plasmid was transfected into HEK293T cells for 48 h. Then cells were treated with 5 μM iridium(III) complexes for 0.5 h at 37 °C. The colocalization of LRP6-GFP and iridium(III) complexes was analyzed by confocal microscopy. The yellow color in the merged images indicate obvious colocalizations of LRP6-GFP with **pbtIrSS** or **ppyIrSS**, while no significant colocalization of LRP6-GFP and **pbtIrOO** or **ppyIrOO** was observed (Figure S28E), suggesting that LRP6 could interact with **pbtIrSS** and **ppyIrSS,** but not **pbtIrOO** and **ppyIrOO**.

Breast CSCs were firstly identified based on the expression of CD44 and CD24. A cell population with high expression of CD44 and low expression of CD24 ($CD44^+/CD24^{-/low}$) has been reported to have stem cell properties, which exhibits enhanced tumorigenesis and metastasis.[18] The $CD44^+/CD24^{-/low}$ cell population was about a 1000 times more tumorigenic than other populations. CD44 is a major target gene of Wnt/β-catenin signaling and considered an attractive target for development of CSC-directed therapeutics.[18c,19] To evaluate the effect of **pbtIrSS** and **ppyIrSS** on breast CSCs, the surface expression of CD44 and CD24 in MDA-MB-231 and MDA-MB-468 cells was detected by flow cytometry. The results revealed that **pbtIrSS** (Figure 5A-F), **ppyIrSS** (Figure S29A-F) and salinomycin (Figure S30A-F) treatment downregulated the surface expression of CD44, enhanced the proportion of $CD44^+/CD24^+$ cells and decreased

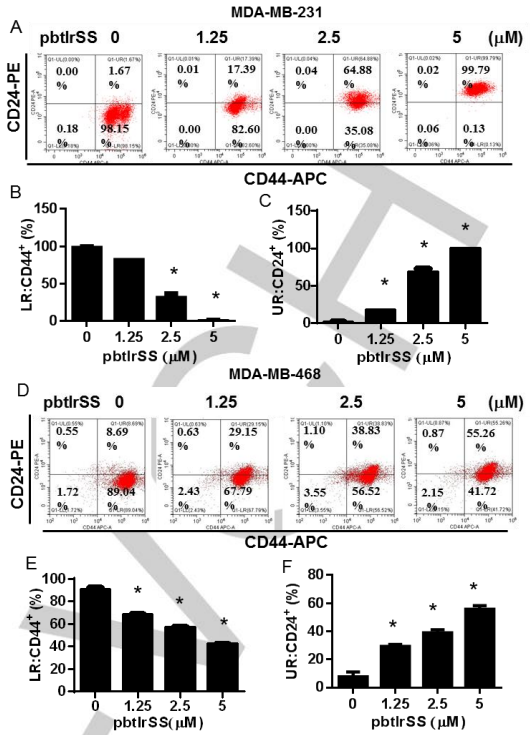

Figure 5. The iridium(III) complex pbtIrSS represses expression of stem cell markers in breast cancer cells. The surface protein expression of CD44 and CD24 was detected by FACS in MDA-MB-231 (A-C) and MDA-MB-468 (D-F) cells treated with **pbtIrSS**. The percentage of CD44 (B and E) and CD24 (C and F) positive subpopulations were presented. Statistical analysis was conducted using one-way ANOVA followed by a Dunnett-t test. *P < 0.05 compared to vehicle control.

$CD44^+/CD24^{-/low}$ cells in both cell lines, whereas cisplatin had no effect on the expression of CD44 and cell subpopulations (Figure S31A-F). Moreover, CD44 protein expression was also decreased in a dose-dependent manner following treatment with **pbtIrSS** (Figure S32A and B), **ppyIrSS** (Figure. S29G and H) and salinomycin (Figure. S30G and H) in both cell lines. These results suggest that **pbtIrSS** and **ppyIrSS** may have the ability to abrogate the stemness properties of breast CSCs.

We next performed a sphere formation assay to examine the effect of **pbtIrSS, ppyIrSS,** salinomycin and cisplatin on CSC self-renewal potential, respectively. The breast cancer Hs578T cells were treated with each complex at 1.25 and 2.5 μM for 10 days. As shown in Figure S33A and B, treatment with **pbtIrSS, ppyIrSS** and salinomycin significantly decreased the number and size of tumor sphere, while cisplatin had no inhibitory effect on sphere formation of breast cancer cells. Importantly, we noted that sulfur-coordinated organoiridium(III) complexes and salinomycin have comparable inhibitory effects on Wnt signaling and breast CSCs.

Concerning about **pbtIrSS** has more potent effects on the biological behaviours of breast cancer cells compared with **ppyIrSS**, **pbtIrOO**, **ppyIrOO** and cisplatin, this complex was further evaluated its anticancer activity *in vivo* by using a MDA-MB-231 cell xenograft model. MDA-MB-231 cells were injected into nude mice subcutaneously. When the tumor volumes reached about 50 mm^3, mice were treated by i.p. injection with saline, cisplatin or **pbtIrSS** at 3 mg/kg on days 0, 3, 6, 9, 12. After treatment for 5 times, mice were sacrificed on the fifteenth day,

10.1002/anie.202015009

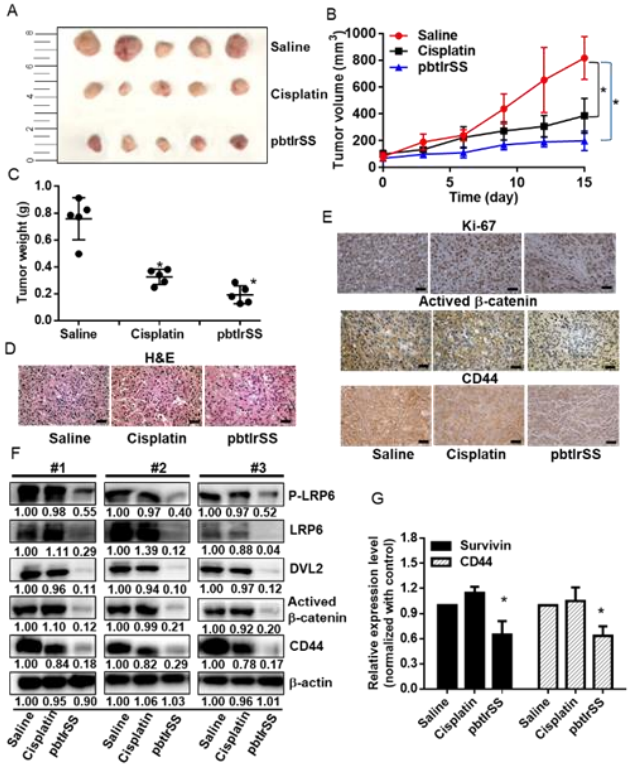

Figure 6. The iridium(III) complex pbtIrSS inhibits tumor growth in a breast cancer xenograft mouse model. MDA-MB-231 xenografts were treated with saline, **pbtIrSS** or cisplatin at 3 mg/kg on days 0, 3, 6, 9 and 12 by i.p. injection. After treatment for 5 times, mice were sacrificed on the fifteenth day, and tumors were excised and weighed. (A) Images of tumors from control group and treatment group. (B) Mean tumor volumes. (C) Mean tumor weight. (D) H&E staining of tumor section; scale bar, 200 μm. (E) IHC staining of Ki-67, β-catenin and CD44; scale bar, 200 μm (F) The expression levels of indicated components of Wnt signaling in tumor samples were visualized by immunoblotting. (G) The mRNA levels of survivin and CD44 were quantitated by real-time PCR. Statistical-analysis was conducted using one-way ANOVA followed by a Dunnett-t test. *P < 0.05 compared to vehicle control.

and tumor volumes and weight were measured. The total RNAs and proteins in the xenografts were extracted, and the histological properties of the tumors were studied. **pbtIrSS** exhibited more potent inhibitory effect on tumor growth *in vivo* than cisplatin (Figure 6A-C). Histological studies indicated that treatment with **pbtIrSS** significantly decreased the tumor cell density (Figure 6D) and expression of the proliferation marker Ki-67 (Figure 6E) compared with vehicle control and cisplatin. In addition, the results of immunohistochemical staining indicated that **pbtIrSS** effectively inhibited the expression of active β- catenin and CD44 in xenograft tumor tissues (Figure 6E). Furthermore, treatment with **pbtIrSS** significantly decreased the protein levels of phosphorylated LRP6, total LRP6, phosphorylated and unphosphorylated DVL2, active β-catenin and CD44 (Figure 6F). The inhibition of **pbtIrSS** towards Wnt signaling were further confirmed by real-time PCR analyses, which exhibited an effective reduction in mRNA expression of Wnt target genes survivin and CD44 (Figure 6G). However, we did not observe any inhibitory effect of cisplatin on the Wnt signaling pathway (Figure 6D-G), suggesting that cisplatin exerts its antitumor activity in a Wnt-independent manner.

Metastasis is a major cause of breast cancer-related death. Blockade of Wnt/β-catenin signaling suppresses breast cancer

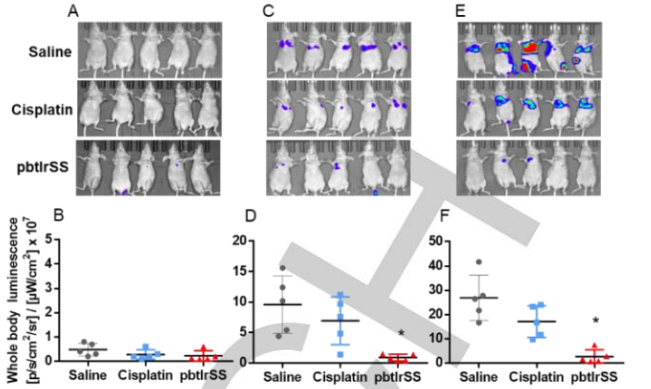

Figure 7. The iridium(III) complex pbtIrSS exerts anti-metastatic activity in lung metastasis mouse model. Experimental lung metastasis mouse model was established by using luciferase-labelled MDA-MB-231 cells. MDA-MB-231-Luc cells were intravenously implanted into the nude mice. On day 25 after injection of breast cancer cells, mice were treated with saline, cisplatin or **pbtIrSS**, respectively, at a dosage of 3 mg/kg for twice a week for two weeks by i.p. Bioluminescence imaging of mice in the control and treatment groups on day 25 (A), day 32 (C) and day 39 (E) after cell injection. The tumor burden was quantitatively expressed as luminescence signal intensity in the region of interest on day 25 (B), day32 (D) and day 39 (F) after cell injection. Statistical analysis was conducted using one-way ANOVA followed by a Dunnett-t test. *P < 0.05 compared to vehicle control.

metastasis by inhibiting CSC-like phenotype.[20] As an antagonistic agent against Wnt/β-catenin signaling, **pbtIrSS** exhibited potent inhibitory effects on the stemness properties, migration and invasion of breast cancer cells. These results strongly suggest that **pbtIrSS** may possess anti-metastasis potential. To validate the anti-metastatic efficacy of **pbtIrSS** *in vivo*, we generated a breast cancer-derived lung metastases model in BALB/c-nu mice. MDA-MB-231 luciferase-expressing cells were injected intravenously into nude mice. Bioluminescence imaging was used to monitor the lung tumor burden. The tumor growth was first detected on day 25 after injection (Figure 7A and B). Then the mice were divided randomly into three groups and treated i.p. with saline, cisplatin or **pbtIrSS** 3 mg/kg twice a week for two weeks. *In vivo* bioluminescent imaging revealed that a significant reduction in metastasis to the lungs in the **pbtIrSS**-treated group compared with the control group and cisplatin-treated group for one week (Figure 7C and D) and two weeks (Figure 7E and F), suggesting that **pbtIrSS** has great anti-metastasis activity in breast cancer *in vivo*.

Conclusion

In summary, four organoiridium(III) complexes **pbtIrSS**, **ppyIrSS**, **pbtIrOO** and **ppyIrOO** were designed and characterized. Among these complexes, **pbtIrSS** and **ppyIrSS** exhibited a novel mechanism for breast cancer therapy for the first time. Both complexes blocked the Wnt/β-catenin signaling cascade by inhibiting LRP6 degradation via a lysosome-dependent manner. We demonstrated that **pbtIrSS** and **ppyIrSS** could potently induce apoptosis and inhibit viability, migration and invasion in breast cancer cells. Moreover, both complexes inhibited sphere formation and mediated stemness properties of breast cancer cells. Importantly, **pbtIrSS** exhibited potent anti-tumor and anti-metastasis activities in breast cancer xenograft models.

Collectively, these results demonstrate that **pbtIrSS** exhibits great anti-breast cancer activity *in vitro* and *in vivo*. This work provides a novel mechanism underlying the inhibition of the Wnt/β-catenin pathway by sulfur-coordinated organoiridium(III) complexes.

Acknowledgements

This work was supported by National Nature Science Foundation of China (Grant No. 81802662, 22077085, 21671137 and 31970739), Nature Science Foundation of Guangdong Province (Grant No. 2017A030310329, 2019A1515011958 and 2020A1515010340), the Shenzhen Peacock Innovation Team Project (Grant KQTD20140630100658078), Shenzhen Basic Research Program (Grant No. JCYJ20170817094611664, JCYJ20190808153209537 and JCYJ20190808173601655), Shenzhen Peacock Plan (Grant No.827000186 and 827000183), SZU medical young scientists program (Grant No. 71201-000001) and Medical Science and Technology Research Foundation of Guangdong Province (Grant No. A2019475). We appreciate the Instrumental Analysis Center of Shenzhen University.

Keywords: Bioinorganic Chemistry • Metals in Medicine • Organoiridium • Wnt/β-catenin signaling • Anti-breast cancer

[1] F. Bray, J. Ferlay, I. Soerjomataram, R. L. Siegel, L. A. Torre, A. Jemal, *CA Cancer J. Clin.* **2018**, *68*, 394-424.

[2] (a) F. Ghasemi, P. Z. Sarabi, S. S. Athari, A. Esmaeilzadeh, *Int. J. Biochem. Cell Biol.* **2019**,*109*, 76-81; (b) M. G. Scioli, G. Storti, F. D'Amico, P. Gentile, G. Fabbri, V. Cervelli, A. Orlandi, Cancers (Basel) **2019**, *11*, 1021.

[3] (a) A. Klaus, W. Birchmeier, *Nat. Rev. Cancer* **2008**, *8*, 387-398; (b) P. Polakis, *Curr. Opin. Genet. Dev.* **2007**, *17*, 45-51.

[4] (a) Y. Wang, M. van der Zee, R. Fodde, L. J. Blok, *Oncotarget* **2010**, *1*, 674-684; (b) F. Ghasemi, P. Z. Sarabi, S. S. Athari, A. Esmaeilzadeh, *Int. J. Biochem. Cell Biol*. **2019**, *109*, 76-81; (c) J. R. Prosperi, K. H. Goss, *Curr. Drug Targets* **2010**, *11*, 1074-1088; (d) M. Kahn, *Semin. Reprod. Med.* **2015**, *33*, 317-325.

[5] (a) B. T. MacDonald, K. Tamai, X. He, *Dev. Cell* **2009**, *17*, 9-26; (b) K. Tamai, X. Zeng, C. Liu, X. Zhang, Y. Harada, Z. Chang, X. He, *Mol. Cell* **2004**, *13*, 149-156; (c) X. Zeng, K. Tamai, B. Doble, S. Li, H. Huang, R. Habas, H. Okamura, J. Woodgett, X. He, *Nature*, **2005**, *438*, 873-877; (d) Y. Duchartre, Y. M. Kim, M. Kahn, *Crit. Rev. Oncol. Hematol.* **2016**, *99*, 141-149.

[6] X. Wang, Z. Guo, *Chem. Soc. Rev.* **2013**, *42*, 202-224.

[7] G. Tallen, C. Mock, S. B. Gangopadhyay, B. Kangarloo, B. Krebs, J. E. Wolff, *Anticancer Res.* **2000**, *20*, 445-449.

[8] (a) H. Y. Huang, P. Y. Zhang, B. L. Yu, Y. Chen, J. Q. Wang, L. N. Ji, H. Chao, *J. Med. Chem.* **2014**, *57*, 8971-8983; (b) F. E. Poynton, S. A. Bright, S. Blasco, D. C. Williams, J. M. Kelly, T. Gunnlaugsson, *Chem. Soc. Rev.* **2017**, *46*, 7706-7756; (c) L. Zeng, P. Gupta, Y. Chen, E. Wang, L. Ji, H. Chao, Z. S. Chen, *Chem. Soc. Rev.* **2017**, *46*, 5771-5804; (d) A. Notaro, G. Gasser, *Chem. Soc. Rev.* **2017**, *46*, 7317-7337; (e) J. Karges, U. Basu, O. Blacque, H. Chao, G. Gasser, *Angew. Chem. Int. Ed.* **2019**, *58*, 14334-14340; (f) S. Kuang, L. L. Sun, X. R. Zhang, X. X. Liao, T. W. Rees, L. L. Zeng, Y. Chen, X. T. Zhang, L. N. Ji, H. Chao, *Angew. Chem. Int. Ed.* **2020**, *59*, 20697-20703; (g) Z. Y. Pan, C. P. Tan, L. S. Rao, H. Zhang, Y. Zheng, L. Hao, L. N. Ji, Z. W. Mao, *Angew. Chem. Int. Ed.* **2020**, *59*,18755-18762; (h) J. Roque III, D. Havrylyuk, P. C. Barrett, T. Sainuddin, J. McCain, K. Colon, W. T. Sparks, E. Bradner, S. Monro, D. Heidary, C. G. Cameron, E. C. Glazer, S. A. McFarland, *Photochem. Photobiol.* **2020**, *96*, 327-339.

[9] (a) L. J. Liu, W. Wang, S. Y. Huang, Y. Hong, G. Li, S. Lin, J. Tian, Z. Cai, H. D. Wang, D. L. Ma, C. H. Leung, *Chem. Sci.* **2017**, *8*, 4756-4763; (b) K. Vellaisamy, G. Li, W. Wang, C. H. Leung, D. L. Ma, *Chem. Sci.* **2018**, *9*, 8171-8177; (c) K. Vellaisamy, G. Li, C. N. Ko, H. J. Zhong, S. Fatima, H. Y. Kwan, C. Y. Wong, W. J. Kwong, W. Tan, C. H. Leung, D. L. Ma, *Chem. Sci.* **2018**, *9*, 1119-1125; (d) J. J. Cao, C. P. Tan, M. H. Chen, N. Wu, D. Y. Yao, X. G. Liu, L. N. Ji, Z. W. Mao, *Chem. Sci.* **2017**, *8*, 631-640; (e) A. H. Day, M. H. Ubler, H. L. Best, E. Lloyd-Evans, R. J. Mart, I. A. Fallis, R. K. Allemann, E. A. H. Al-Wattar, N. I. Keymer, N. J. Buurma, S. J. A. Pope, *Chem. Sci.* **2020**, *11*, 1599-1606; (f) T. L. Lam, K. C. Tong, C. Yang, W. L. Kwong, X. Guan, M. D. Li, V. Kar-Yan Lo, S. Lai-Fung Chan, D. Lee Phillips, C. N. Lok, C. M. Che, *Chem. Sci.* **2019**, *10*, 293-309; (g) V. Venkatesh, R. Berrocal-Martin, C. J. Wedge, I. Romero-Canelon, C. Sanchez-Cano, J. I. Song, J. P. C. Coverdale, P. Zhang, G. J. Clarkson, A. Habtemariam, S. W. Magennis, R. J. Deeth, P. J. Sadler, *Chem. Sci.* **2017**, *8*, 8271-8278.

[10] H. Huang, S. Banerjee, K. Qiu, P. Zhang, O. Blacque, T. Malcomson, M. J. Paterson, G. J. Clarkson, M. Staniforth, V. G. Stavros, G. Gasser, H. Chao, P. J. Sadler, *Nat. Chem.* **2019**, *11*, 1041-1048.

[11] M. H. Chen, Y. Zheng, X. J. Cai, H. Zhang, F. X. Wang, C. P. Tan, W. H. Chen, L. N. Ji, Z. W. Mao, *Chem. Sci.* **2019**, *10*, 3315-3323.

[12] Y. Hisamatsu, N. Suzuki, A. A. Masum, A. Shibuya, R. Abe, A. Sato, S. I. Tanuma, S. Aoki, *Bioconjug. Chem.* **2017**, *28*, 507-523.

[13] K. Laws, A. Eskandari, C. Lu, K. Suntharalingam, *Chem.-Eur. J.* **2018**, *24*, 15205-15210.

[14] (a) W. Lu, Y. Li, *J. Cell Biochem.* **2014**, *115*, 1799-1807; (b) H. An, J. Y. Kim, N. Lee, Y. Cho, E. Oh, J. H. Seo, *Biochem. Biophys. Res. Commun.* **2015**, *466*, 696-703.

[15] (a) C. Niehrs, *Oncogene* **2006**, *25*, 7469-7481; (b) A. Ehrlund, N. Mejhert, S. Lorente-Cebrian, G. Astrom, I. Dahlman, J. Laurencikiene, M. Ryden, *J. Clin. Endocrinol. Metab.* **2013**, *98*, E503-508; (c) N. Krishnamurthy, R. Kurzrock, *Cancer Treat. Rev.* **2018**, *62*, 50-60.

[16] L. Zhou, Z. Wang, S. Yu, Y. Xiong, J. Fan, Y. Lyu, Z. Su, J. Song, S. Liu, Q. Sun, D. Lu, *J. Pharmacol. Exp. Ther.* **2020**, *373*, 149-159.

[17] J. Zhang, Y. Li, Q. Liu, W. Lu, G. Bu, *Oncogene* **2010**, *29*, 539-549.

[18] (a) W. Li, H. Ma, J. Zhang, L. Zhu, C. Wang, Y. Yang, *Sci. Rep.* **2017**, *7*, 13856; (b) S. Ricardo, A. F. Vieira, R. Gerhard, D. Leitao, R. Pinto, J. F. Cameselle-Teijeiro, F. Milanezi, F. Schmitt, J. Paredes, *J. Clin. Pathol.* **2011**, *64*, 937-946; (c) C. Sheridan, H. Kishimoto, R. K. Fuchs, S. Mehrotra, P. Bhat-Nakshatri, C. H. Turner, R. Goulet, Jr. S. Badve, H. Nakshatri, *Breast Cancer Res.* **2006**, *8*, R59.

[19] A. DA C. Paula, C. Lopes, *Anticancer Res.* **2017**, *37*, 2173-2183.

[20] G. B. Jang, J. Y. Kim, S. D. Cho, K. S. Park, J. Y. Jung, H. Y. Lee, I. S. Hong, J. S. Nam, *Sci. Rep.* **2015**, *5*, 12465.

10.1002/anie.202015009

Entry for the Table of Contents

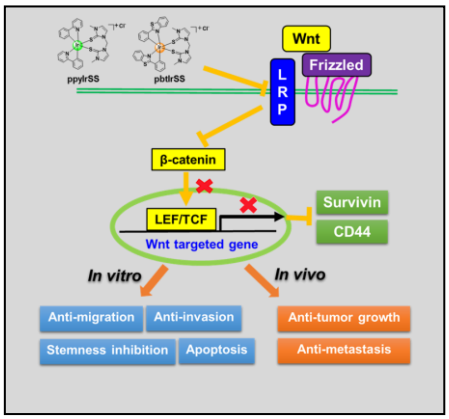

Sulfur-coordinated organoiridium(III) complexes were explored their effects on Wnt/β-catenin signaling, apoptosis, migration, invasion and stemness in breast cancer cells for the first time. The results demonstrated that **pbtIrSS** exerted great anti-tumor and anti-metastatic activities in breast cancer cells via inhibiting Wnt/β-catenin signaling and CSCs.